2008
20th International Lightning Detection Conference
21-23 April • Tucson, Arizona, USA
2nd International Lightning Meteorology Conference
24-25 April • Tucson, Arizona, USA

THE USE OF IMPULSE CHARGE MOMENT CHANGES TO PREDICT SPRITES IN MESOSCALE CONVECTIVE SYSTEMS

Walter A. Lyons, CCM, Jonathan Meyer and Thomas E. Nelson
FMA Research, Inc
Fort Collins CO 80524

Steven A. Rutledge and Timothy L. Lang
Colorado State University
Fort Collins, CO 80523

Steven A. Cummer
Duke University
Durham, NC 27708

1. INTRODUCTION

The serendipitous discovery of red sprites in 1989 changed forever our view of the interactions between tropospheric electrical activity and middle atmospheric optical phenomena and energetics (Franz et al. 1990; Lyons and Armstrong 2004). Once thought to be electrically quiescent, the stratosphere and mesosphere are increasingly found to be the home to a growing variety of lightning-related electrical discharges and intense transient electric fields (Lyons 2006; Lyons et al. 2003a). The discovery of literal cloud-to-stratosphere electrical discharges from intense thunderstorm tops, including blue jets, giant jets and true upward lightning (Lyons et al. 2003b; van der Velde et al. 2007) continues to engender the need for intensive investigations of this region. However, the relative scarcity and apparently random nature of cloud top discharge events make them difficult to study in a systematic manner. Red sprites, and to a lesser extent elves (Fukunishi et al. 1996) and halos (Barrington-Leigh 1999), by contrast, are increasingly well understood and predictable.

During the summer of 2000, a major field program, the Severe Thunderstorm Electrification and Precipitation Study (STEPS) was conducted on the U.S. High Plains (Lang et al. 2004). While its focus was on supercell convection, the experimental design also allowed for detailed investigations of mesoscale convective systems (MCSs). Over continental regions, sprites are known to frequently occur in association with positive cloud-to-ground (+CG) strokes in MCSs (Lyons 1994, 1996; Lyons et al. 2000), although even in the most productive storms rarely do more than 1 in 5 +CGs trigger a sprite. During STEPS, though an occasional sprite was recoded from supercellular storms (Lyons et al. 2008), the vast majority of sprites and halos were observed above large mesoscale convective systems (Lyons et al. 2003a).

Theoretical research into red sprite production has seen the proposal and disposal of a number of theories (Wilson 1925; Rodger 1999). At the current time, sprites are generally agreed to be the result of conventional dielectric breakdown at approximately 70-75 km height (Stanley 2000), the result of a strong transient electrical field resulting from the removal to ground of large amounts of electrical charge in a CG flash (Pasko et al. 1996, 1998). Though this mechanism is not strongly polarity dependent, the vast majority of sprite parent CGs are positive (SP+CGs), with only two documented –CG events by Barrington-Leigh et al. (1999) and several in Argentina by Bailey et al (2007). While the peak current of SP+CGs is typically 50% larger than the other +CGs in the same storm (Lyons et al. 2003b; Lyons 1996), the peak current by itself is not a good predictor of sprite formation. As initially suggested by C.T.R. Wilson (1925), the key metric is the charge moment change:

$$\Delta M_q(t) = Z_q \times Q(t) \quad (1)$$

defined as the product of Z_q, the mean altitude (AGL) from which the charge is lowered to ground, and the amount of charge lowered. Note that this second term is most appropriately considered as a function of time. New measurement techniques (Cummer and Lyons, 2004, 2005) can now routinely monitor the impulsive charge moment change (iΔM_q), which is that produced by the charge lowered in roughly the first 2 ms of the CG. This is often dominated by the return stroke plus the initial stages of any continuing current.

Huang et al. (1999) and Williams (2001) refined Wilson's original theory and proposed, based upon initial measurements gleaned from Schumann resonance ELF transient analyses (Boccippio et al. 1995), that for such breakdown to occur, total ΔM_q values would need to be on the order of 300 to 1000 C km. These values are many times larger than what have been believed to be the "normal" values for ΔM_q (Rakov and Uman 2003). The STEPS program provided ideal circumstances to delve into the characteristics of MCS SP+CGs strokes (Lyons et al. 2003a; Lyons et al. 2008). The key question that was addressed: What is different about those +CGs which trigger sprites? Where in the storms, and during what phase of its life cycle, do these unusual discharges occur? It became clear that a large charge moment change was indeed a robust sprite predictor, and a necessary if not sufficient condition. Though variability in critical threshold may occur from night to night (Cummer and Lyons 2004), a total ΔM_q value of ~500 C km appears to be a reliable metric, and is usually achieved (in about 50% of sprites) after ~10 ms of the return stroke (with variability ranging from <1 ms to > 100 ms. The occurrence of long delayed sprites clearly point towards the role of continuing currents in +CGs as a major factor in the production of the majority of sprites. The database amassed during STEPS allowed for the creation of criteria for MCS sprite production based upon the size and temperature of the cloud top canopy and the size and character of the underlying radar reflectivity pattern. TLEs occur infrequently in summer season MCSs with cloud temperatures everywhere warmer than -55°C. Most TLEs also require peak reflectivities within the parent MCS be >55 dBZ. Reported upon in detail by Lyons et al. (2006a,b), these criteria have been incorporated into successful qualitative, and more recently, an automated TLE-potential forecasting system. It should be noted that these criteria apply primarily to mid-latitude, warm season, continental convective systems. If met, these criteria suggest the storm is likely producing CGs with large ΔM_q values, primarily in the trailing stratiform region. Figure 1 is a matrix, which summarizes the state-of-the-science with respect to TLE-potential for various convective regimes. Virtually any storm producing lightning can generate a discharge with a ΔM_q value sufficient to cause mesospheric breakdown, However, it appears some regimes are far more efficient than others at this task. A major research thrust continues to be the expansion of the parameter space for convective regimes generating sprite-producing lightning. Clearly the TLE prediction rules for U.S. High Plains convection will not apply to cold season, shallow convective storms such as found over the Gulf Stream, sometimes the Great Lakes and the Sea of Japan.

RF-based remote sensing methods for the characterization of lightning charge moment changes based upon the concepts proposed by Cummer and Inan (2000), and as exploited for STEPS data by Cummer and Lyons (2004, 2005) has detailed that ΔM_q and even iΔM_q (if properly employed) can provide a very useful threshold to discriminate between those +CGs which produce sprites (and elves and halos) and those which do not. In this paper we will investigate the characteristics of TLE-producing storms as observed using conventional NLDN data (Cummins et al. 1998), GOES satellite and NEXRAD radar reflectivity, a 3-D lightning mapping array (LMA) (Thomas et al. 2004) and impulse charge moment change data automatically extracted in real-time using ULF/ELF/VLF transient analysis. This technique forms the basis of a national Charge Moment Change Network (CMCN) that has been operating since early 2007 as part of ongoing sprite forecasting and verification activities.

2. IMPULSE CHARGE MOMENT CHANGES

TLE research has advanced largely due to the ability of LLTV systems to detect luminosity above storms during the dark of night. However, it is clearly desirable to have a surrogate that can work throughout the diurnal cycle, as well as when clouds block the view of ground cameras. From several studies (Hu et al 2002; Lyons et al 2003b) it appears that a relatively narrow threshold range of ΔM_q values exists to allow discriminating those CGs which do and do not produce sprites, halos and elves. The extraction of the full (10 ms or longer) ΔM_q value from ULF/ELF/VLF transient data is still a rather laborious task, which currently limits the extent of both case studies, and especially any potential operational utilization of this parameter. Recent advances in the extraction of the impulse ΔM_q values (Cummer and Lyons, 2004, 2005) suggested that an automated approach was feasible. The question then arose as to whether the impulse iΔM_q contains sufficient predictive value to be a useful discriminator for sprites (high probability of detection, low false alarm rate). Unless the iΔM_q value exceeds the nominal 500 C km breakdown threshold, there is no *a priori* reason to expect this parameter to be a predictor of sprites triggering more than 2 ms after the CG return stroke.

Initial tests with Duke University conducted in conjunction with LLTV monitoring of MCSs from YRFS during the summer of 2005 and reported upon in Lyons et al. (2006a,b) revealed that iΔM_q values exhibit a surprisingly high predictive value for both short and long-delayed sprites. Tests demonstrated that a nominal threshold value of 100 C km (in the first 2 ms of the event) produced a >50% probability of detection (PoD) of the sprites, halos, trolls and elves as confirmed by image-intensified cameras over High Plains convective storms. Moreover, false alarm rates were small. During the summer of 2005, a major field campaign entrained investigators from other institutions, resulting in a large database for further testing the relationships between CG lightning RF signatures, their parent storms' distinguishing features, and TLEs. A more sensitive receiver, spanning ULF/ELF/VLF frequencies, yielded even higher TLE detection efficiencies for individual TLE parent CGs (>60% in a large mesoscale convective system [MCS]), virtually assuring that TLE-producing storms can be identified. By enhancing the Duke algorithms to employ the ULF signal component and automating the extraction processes, the technique held promise to develop a real-time system to distinguish those CGs which produce truly extraordinary stratospheric electric fields triggering mesospheric breakdown. Given an anticipated useful range of 1500 km or better, only two receivers appeared required to create a prototype quasi-national Charge Moment Change Network (CMCN) for real-time TLE monitoring. The unique iCMC data (a measure of the electrical charge lowered to ground not now operationally observed), would appear to have significant potential for use in electrical engineering, lightning protection design studies, forest fire detection, forensic and insurance investigations and atmospheric research.

The investigation of the utility of using real-time iΔM_q data as a surrogate for TLE detection was the focus of the SPRITES 2007 program.

3. SPRITES 2007

The SPRITES 2007 campaign was headquartered at YRFS during May through August. Monitoring by LLTV cameras, as in past years, detected numerous TLEs at ranges to 500 km and beyond. Additional experiments were conducted with Stanford University's STAR Lab in which the ability to predict the time and location of TLE-producing storm was essential (Fig. 2). The 2007 campaign marked the inauguration of the CMCN. The first sensor cam eon line at Duke University (Durham, NC) in early February 2007, and was joined by a second sensor ay YRFS in early June. Figure 3 shows the highly sensitive orthogonal magnetic coils that were deployed beneath "fake rock" enclosures in radio quiet environments. A variable threshold trigger was adjusted until such time as the local noise would not overwhelm local PC processing capability. Information on candidate waveform signatures were sent from both sensors to a central processing facility at Duke. The automated extraction routine produced a continuous stream of GS-time tagged iΔM_q estimates. Once the magnitude was ascertained, there remained the matter of geolocating the event. While single and multi-station techniques exist to approximately locate the origin of these energetic events, it was deemed most practical to use the NLDN data stream on CGs to locate the events by time matching events down to the microsecond level (with appropriate care taken for propagation delays, etc.). This approach, however, is dependent upon the NLDN's capability to detect the sprite parent CG. Experience has shown that the detection efficiency for these events may be somewhat lower than for +CGs as a whole, perhaps due to the complicated waveform patterns involved or signal strength so large as to saturate many receivers.

A real time display of iΔM_q estimates is shown in Fig. 4. The CMCN can detect the iΔM_q value from "normal" CGs, typically well under 25 C km. For purposes of TLE monitoring, however, the displays were designed just to show larger events, starting with an arbitrary threshold of 75 C km, and also those events 100-300 C km, and the largest events, > 300 C km. Both positive (red) and negative (blue) iΔM_q estimates are plotted on a 3-hour summary chart, updated every 5 minutes. Typically large (> 100 C km) positive events greatly outnumber the negative events, especially above 300 C km. But a surprisingly large number of negative iΔM_q readings > 100 C km have been noted.

Moreover, initial experience has shown substantial patterning in $i\Delta M_q$ reports by polarity, with many storms exhibiting structures reminiscent of the "bipolar" patterns first noted when NLDN became widely available (Engholm et al. 1990). It quickly became apparent from experience that when displays indicted + $i\Delta M_q$ > 300 C km, there was a very high probability of sprites being produced by the parent storm.

Figure 5 shows the sprites and halos that were optically confirmed by LLTVs during 2007 and geolocated by pairing them with the SP+CGs in the NLDN database. (Two events in Missouri are actually gigantic jets detected by automated cameras and reported by van der Velde et al. [2007]). One may note that the 2007 map reports TLEs far beyond the maximum 1000 km range of the LLTV at YRFS. A second major activity for SPRITES 2007 was establishing a Sprite Net of volunteers supplied with LLTV cameras and provided with daily forecasts and email updates as to potential targets. The CMCN displays proved to be exceptionally useful at identifying target TLE-producing storms for LLTV monitoring. The first sprites along the east coast and the upper Great Lakes have been reported. Also the CMCN alerted YRFS operators to point cameras to the northwest (for the first time ever) in order to record the first sprites over the western mountainous region of Wyoming. (In January, 2008, the CMCN similarly alerted the Duke camera operators to capture the first sprites over the Gulf Stream, confirming the predictions by Price et al. [2002].)

Figure 6 shows the nominal 500 km detection range of the six Sprite Net cameras. Forecast guidance was also provided by developing a display system in which the NAM WRF model output was converted into an emulation of the color-coded IR GOES images (blue = -50°C, green = -60°C and red = -70°C) used to evaluate whether a given MCS met the criteria developed during STEPS. Using simulated NEXRAD reflectivity predictions from the NAM WRF, a detailed prognostic system for TLE-producing storms out to 72 hours has been developed and will be the topic of future papers.

These new capabilities are rapidly allowing us to explore TLE production in a widening variety of storm types. As confidence is gained in the CMCN-derived $i\Delta M_q$ estimates to serve as surrogates for sprites, investigations into the climatology and meteorology of sprites will begin to make rapid advances. This will initially take place with a series of detailed case studies. We herein provide one such analysis, but we will begin with the "classic" TLE-producing system, the largest of the MCSs, a mesoscale convective complex (MCC), characterized by an intense leading convective core and a large trailing stratiform region with a distinct bright band signature that evolved over many hours of time.

4. 20 JUNE 2007: A PROTOTYPICAL TLE-PRODUCING MCS

Figure 7 shows the synoptic pattern at 0600 UTC on 20 June 2007. A flow of extremely moist, unstable air into Texas and Oklahoma began interacting with a weak low pressure area and stationary front. Late the previous afternoon, a supercell formed in Kansas and moved south into an area of extreme CAPE (3000 - 5000 J kg^{-1}) over Oklahoma and Texas (Fig. 8). Another system grew into an MCS and moved eastward out of the Texas Panhandle. These systems merged, rapidly evolved upscale, and became a large mesoscale convective system, which by 0600 UCT covered a vast area (652,000 km^2 at –50°C) (Fig. 9). The copious supply of low-level moisture feeding the system is evident in Fig. 10. If one were to consult a summary display of NLDN reports, such as that shown in Fig.11, the vast number of CGs (and ICs) would be evident, though little information on any patterning or structure in the various lightning parameters could be gleaned. The CMCN real-time display, however, clearly showed a large area of very large + $i\Delta M_q$ events in western and northern Oklahoma, with some negative $i\Delta M_q$ events as well present in the eastern part of the MCC (Fig. 12). One may note by comparison with the NLDN display, not all storms necessarily produce many, or any, $i\Delta M_q$ events > 75 C km, even over extended periods of time.

Light winds aloft were typical of conditions favoring the nocturnal MCCs that frequent this region. The MCC continued surging southward and expanding through the night with an extremely large area of high, cold cloud tops. There was a classic bright band/secondary precipitation maximum over the Oklahoma LMA as depicted on the 0605 UTC NEXRAD radar mosaic (Fig. 13). The Oklahoma LMA was ideally situated to provide detailed investigations of both the macroscale lightning patterns and for many individual discharges (Fig. 14). This MCC was perhaps the largest MCS of the season in the central U.S., as suggested by the cloud canopy display in Fig. 15a,b. By plotting both the NLDN-detected CGs and ICs one notes the typical pattern of very high lightning densities of both polarities, but especially negative discharges, in the leading line convective cores, with widespread but lower density events in the trailing stratiform, of mostly positive polarity. This basic bipolar pattern remained quasi-steady state for 4 to 6 hours, although with positive CGs tending to concentrate more rearwards in the trailing stratiform as the night wore on. A typical 5 minute sample of NLDN data at 0600 UTC shows that large peak current (>75 kA) negative CGs were concentrating within the leading line convective cores, whereas the large peak current positives had migrated largely into the trailing stratiform (Figure 16). Figure 17 shows the large peak current +CGs tended to be associated with the trailing secondary precipitation maximum and relatively low echo top regions in the WDT, Inc. regional mosaic. A summary of all 15,350 positive and 252,765 negative CGs (> 10 kA) between 0000 and 0800 UTC are shown in Fig. 18. This storm was clearly predominately negative CG dominated (94%) throughout its life cycle. However, as will become clear, the characteristics of some +CGs in the trailing stratiform account for the vast number of sprites observed. As shown in Figure 19, even over an eight hour period, there is a clear spatial sorting of large peak current CGs (> 75 kA) of both polarities, with positives in the trailing stratiform and negatives towards the leading (eastern and southern) edge.

Figure 20 shows the positions of those 233 SP+CGs detected by the NLDN with optically confirmed sprites. A total of 282 sprites were imaged by the LLTV camera. In this case, about 18% of the SP+CGs went undetected by the NLDN (assuming all sprites indeed have parent +CGs). We note that 111 of the NLDN detected SP+CGs were within 200 km of the centroid of the Oklahoma LMA. Very little cloud blockage hindered the YRFS cameras, though there seemed to be some haze and/or smoke that may have limited seeing a bit (from a western slope fire?). Along the LLTV camera line of sight, light pollution from nearby Windsor, CO may have made some dim events harder to see. Generally sprites were flat and wide (smudges or comb type), and most were not that bright (inherently dim or attenuation by smoke?) Even with these impediments, many TLEs were detected at ranges >700 km. YRFS viewing began at dusk (0300 UTC) and terminated at 0700 UTC as the MCS began to move out of camera range. The Sprite Net Watec 902U H camera system, automated with UFOCapture software, appeared to be working very well with over 250 triggers, roughly the number of sprites observed. (We note, however, that all detailed TLE studies still best relay on manual field-by-field analysis of video tapes).

Figures 21-24 detail the hourly progression of the CG lightning, including those with confirmed sprites, and the + $i\Delta M_q$ events with confirmed sprites during the period of LLTV monitoring, 0300 to 0700 UTC. The CMCN output consistently detected 50 to 65% of those NLDN-detected CGs with confirmed optical sprites. The large majority of the $+i\Delta M_q$ values were above 100 C km, with many > 300 C km. While a few sprites appeared associated with $+i\Delta M_q$ values < 100 C km, we suspect this may be due to assigning parent status to a secondary and lower peak current +CG associated with the horizontally extensive spider lightning discharge which often drops multiple +CGs separated by tens of kilometers. Thus, while the CMCN has a detection efficiency for sprites on the same order of the flash detection efficiency of the pre-1994 NLDN, as with that system, a TLE-producing storm is highly unlikely to go undetected. Also evident is that the + $i\Delta M_q$ events creating sprites were strongly concentrated deep into the trailing stratiform region of the MCC. The occasional sprite near or in the convective core tended to be dim with smaller $i\Delta M_q$ values.

No TLE was able to be definitively associated with a negative $i\Delta M_q$ event. However, there were a number of events >100 C km, and even a very few approaching 300 C km during the period of LLTV observations. As shown in Figure 25, during the 0600-0700 UCT period, most negative $i\Delta M_q$ events >100 C km were concentrated in the convective cores at the leading edge of the MCC. This pattern was consistent throughout the analysis period.

The distribution of retrieved + $i\Delta M_q$ events for confirmed sprites is shown in Figure 26. While, as mentioned, a few (21) events were reported at <100 C km, the remainder were substantially larger than “normal” +CG $i\Delta M_q$ values (< 50 C km), with one attaining 1024 C km. Figure 27 tabulates all + $i\Delta M_q$ events within the storm area during the LLTV observation period. Of the 40 largest values (430 to 1024 C km), fully 75% had an optically confirmed TLE. It is likely some of the “misses” were, in fact, due to a failure of the optical system to detect the dimmer TLEs as a result of the not quite optimal seeing at the extreme ranges being worked this night.

Thus, initial estimates suggest that + $i\Delta M_q$ values provided a Probability of Detection for TLEs that is very encouraging and indeed quite useful. (We plan to examine False Alarm Rates as this study progresses).

Initial analyses of the total lightning discharges using the Oklahoma LMA have produced some interesting results. As shown in Fig. 28, for most of the storm’s life cycle, there existed a bi-level structure consistent with a normal dipole (Carey et al. 2005), with some suggestion of a third layer of positive charge at 4-5 km near the melting layer. We have begun examination of the individual discharges involved in TLE production and will report in detail in a later paper. However, unlike in earlier STEPS studies (Lyons et al. 2003a), in which the in-cloud component of the SP+CG remained largely in the melting layer (around 4 km AGL), a number of events were discovered in which the lightning initiated in the stratiform region near the melting layer, but then migrated upwards to 8-10 km AGL. If this were a consistent pattern, then many +CGs occurred with vertical channel lengths more than twice that postulated by Williams (1998) and seemingly confirmed by Lyons et al. (2003a). This has one immediate implication. This storm produced sprites at a very fast rate, even considering its size and intensity. We have from time to time in the past noted MCSs that produced many more sprites than their peers. Perhaps the advantage of longer vertical channels for CGs is sufficient to push a large number of marginal +CGs over the $i\Delta M_q$ threshold and thus allow for TLEs. This area clearly requires further investigation.

Again, while the LMA analyses are still very preliminary, we have also found that the parent discharges of sprites can begin both in the stratiform and near or in the convective line, and then migrate rearwards into the trailing stratiform before launching a +CG. Such discharge behavior has been noted in previous studies (Lang et al. 2004). Of interest is whether the initiating point of these discharges affects TLE production or continuing current characteristics in any systematic manner.

One SP+CG has proven to be truly extraordinary (Figures 29 - 30). After initiating around 10 km AGL above the rear flank of the convective core, it then built backward and downward into the stratiform region. That in itself is fairly common, but the in-cloud discharge meandered for almost 300 km over a nearly six second duration, spawning two +CGs and sprites near the end of the discharge. The sprites were located to the rear of the trailing stratiform, well removed from the initiation point. This example was chosen at random, and brief inspection of other SP+CGs using the Oklahoma LMA has revealed numerous other discharges >100 - 150 km in length.

5. DISCUSION AND CONCLUSIONS.

In High Plains MCSs during spring through autumn, +CGs producing sufficiently large $i\Delta M_q$ values inducing TLEs typically occur (1) in the trailing stratiform region, (2) associated with radar reflectivities of 20-45 dBZ, (3) in radar echo (>10 dBZ) regions covering >20,000 km^2, (4) in storms which a peak core reflectivity >55dBZ, (5) beneath the colder though not usually the coldest tops, and (6) generally in systems with a maximum cloud top temperature of -55°C or less and –50°C canopy areas of >25,000 km^2.

The observation that sprites rarely occur during the active phase of High Plains supercells, even though they produce copious numbers of high peak current +CGs has been documented. The occasional "end-of-storm" sprites occur when the supercell is developing quasi-MCS stratiform region characteristics (Lyons et al. 2008) and +CGs likely develop longer and/or more intense continuing currents.

Our new capabilities provided by the Sprite Net cameras to routinely monitor different convective regimes in various geographical regions will begin to expand our detailed understanding of TLE production for many of the categories listed in Figure 1.

The extraction of $i\Delta M_q$ values in real-time from ULF/ELF/VLF transient analysis provides additional metrics by which the electrical activity of convective storms can be characterized (Cummer and Lyons 2004, 2005). At a practical level, detection of $i\Delta M_q$ >300 C km virtually assures detection of TLEs by LLTVs out to ranges approaching 700-1000 km (assuming the intervening line of sight is clear).

The "polarity paradox" discussed by Williams et al. (2007) finds that globally far less than 1% of TLEs observed from land cameras occur with negative CGs, while 10x that number of threshold-exceeding ΔM_q events are indicated by global ELF analyses.

Over the U.S. High Plains, in the storms investigated to date, negative CGs have simply not produced large enough ΔM_q values to induce TLEs. The mystery may in part be resolved by noting the large number of high peak current (and large EMP) -CGs over salt water (Lyons et al. 1998). Recent analyses of ISUAL satellite measurements have found very large percentages of halos and elves, also with relatively large charge moment changes, from negative CGs over oceans (Frey et al. 2007).

The results of this study introduce another variant of the polarity paradox. The iΔM_q values reported herein show fewer, but still significant, numbers of negative iΔM_q values > 100 C km, yet none associated with confirmed TLEs. By contrast, the probability of TLEs being reported from positive CGs rises rapidly once iΔM_q value exceed 100 C km. Some (24) of the TLEs appear to be triggered by +iΔM_q values >500 C km. In these cases, the impulse values recorded in 2 ms are sufficient to trigger mesospheric breakdown. The remaining events must apparently rely upon substantial continuing currents to attain the ΔM_q threshold of ~500 C km during a period of time often extending beyond 10 ms after the return stroke. As illustrated in Fig. 31, it appears that while many CGs of both polarities can have iΔM_q values in the 100 to 300 C km range in U.S. High Plains storms, the continuing currents in -CGs (which are fairly common and can extend beyond 100 ms based upon informal analysis of video) almost never are of sufficient intensity to allow further significant accumulation of charge moment change. We do note at least one optically confirmed negative sprite has been recently reported above an Argentine MCS triggered by a CG with a -iΔM_q value of 503 C km (Bailey et al. 2007). We suggest that this event may be from a rare land -CG in which the impulse charge moment change was sufficient to initiate mesospheric breakdown.

The emergence of high-speed video imaging of lightning and sprites (Samaras and Lyons 2008; Cummer et al. 2006) may provide a useful tool to further explore polarity paradox issues. As shown in Fig. 32, a number of details about the lightning discharge are now available for quantitative analysis, including the speed of stepped and dart leaders and the newly recognized recoil streamers in +CGs. Digital high-speed video also provides an excellent means to study both qualitatively and quantitatively the continuing currents in return strokes of both polarities. In addition, earlier 1000 fps video of +CGs suggested numerous pulsations in channel luminosity (perhaps as new pockets of cloud charge are tapped by outspreading spider lightning in-cloud discharges) similar to M-components in –CGs. In +CGs, they are often longer in duration and longer delayed after the return stroke. Yashunin et al. (2007) have suggested such +CG M-component-like pulsations may be causative of some long delayed sprites.

Even more intriguing is the likelihood that the current CMCN ULF/ELF/VLF sensors can provide information from which it is possible to extract the full time dependent charge movement change and the magnitude and duration of continuing currents. This will be an area of active future research.

6. ACKNOWLEDGMENTS

This work has been supported by the National Science Foundation, Physical Meteorology and Aeronomy Programs (ATM-0221512 and ATM-0649034). Partial support of the Duke University effort was from NASA grant NAG5-10270 and from NSF. Nicolas Jaugey's contributions to the CMCN installation and operation are enthusiastically acknowledged. The Oklahoma LMA data and assistance in its interpretation were graciously provided by Don MacGorman. We gratefully acknowledge many useful exchanges with Earle Williams, Mark Stanley and Kenneth Cummins (Vaisala, Inc.). Special thanks to the institutions which hosted Sprite Net camera systems: Minnesota State University, Mankato (Cecil Keen, Josh Jans), Duke University (Nicolas Jaugey), Florida Institute of Technology (Joe Dwyer, Ziad Saleh), Texas A&M (Joe Jurecka, Richard Orville) and the University of Oklahoma (William Beasley). Thanks to Tim Samaras and Tom Warner for their pioneering efforts to obtain high-speed imagery of +CGs.

7. REFERENCES

Bailey, M., M.J. Taylor, P.D. Pautet, S.A. Cummer, N. Jaugey, J.N. Thomas and R.W. Holzworth, 2007: Sprite halos and associated lightning characteristics over South America. AGU Fall Meeting, AE23A-0896, Abstract only.

Barrington-Leigh, C.P., U.S. Inan, M. Stanley and S.A. Cummer, 1999: Sprites directly triggered by negative lightning discharges. *Geophys. Res. Lett.,* **26**, 3605-3608.

Boccippio, D.J., E.R. Williams, W.A. Lyons, I. Baker and R. Boldi, 1995: Sprites, ELF transients and positive ground strokes. *Science*, **269**, 1088-1091.

Carey, L.D., M.J. Murphy, T.L. McCormick and N.W.S. Demetriades, 2005: Lightning location relative to storm structure in a leading-line, trailing-stratiform mesoscale convective system. *J. Geophys. Res.*, **110**, D03105m doi: 10.1029/2003JD004371.

Cummer S.A., N. Jaugey, J. Li, W.A. Lyons, T.E. Nelson and E.A. Gerken, 2006: Submillisecond imaging of sprite development and structure. *Geophys. Res. Lett.,* **33**, L04104, doi: 0.1029/2005GL024969.

Cummer, S.A. and W.A. Lyons, 2005: Implications of lightning charge moment changes for sprite initiation. *J. Geophys. Res*., **110**, A04304, doi:10.1029/ 004JA010812.

Cummer, S.A. and W. A. Lyons, 2004: Lightning charge moment changes in U.S. High Plains thunderstorms. *Geophys. Res. Lett.,***31**, L05114, doi10.1029/ 003GL019043,2004.

Cummer, S.A. and U.S. Inan, 2000: Modeling ELF radio atmospheric propagation and extracting lightning currents from ELF observations. *Radio Science,* **35,** 385-394.

Cummins, K.L., M.J. Murphy, E.A. Bardo, W.L. Hiscox, R.B. Pyle and A.E. Pifer, 1998: A combined TOA/MDF technology upgrade of the U.S. National Lightning Detection Network. *J. Geophys. Res*., **103(D8**), 9035-9044.

Engholm, C., R. Dole and E.R. Williams, 1990: Meteorological and electrical conditions associated with positive cloud-to-ground lightning. *Mon. Wea. Rev.,* **118***,* 470-487.

Franz, R.C., R.J. Nemzek, and J.R. Winckler, 1990: Television image of a large upward electrical discharge above a thunderstorm system. *Science, **249**,* 48-51.

Frey, H.U., S.B. Mende, S.A. Cummer, J. Li, T. Adachi, H. Fukunishi, Y. Takahashi, A.B. Chen, R.-R. Hsu, H.-T. Su and Y.-S. Chang, 2007: Halos generated by negative cloud-to-ground lightning. *Geophys. Res. Lett.,* **34,** L18801, doi: 10.1029/2007GL030908.

Fukunishi, H., Y. Takahashi, M. Kubota, K. Sakanoi, U.S. Inan and W.A. **Lyons**, 1996: Elves, Lightning-induced transient luminous events in the lower ionosphere. Geophys. Res. Lett. 23, 2157-2160.

Hu, W., S. Cummer, W.A. Lyons and T. E. Nelson, 2002: Lightning Charge Moment Changes for the Initiation of Sprites," *Geophys. Res. Lett., **29**,* 10.1029/2001GL014593.

Huang, E., E. Williams, R. Boldi, S. Heckman, W. Lyons, M. Taylor, T. Nelson and C. Wong, 1999: Criteria for sprites and elves based on Schumann resonance observations. *J. Geophys. Res.,* **104,** 16943-16964.

Lang, T, L. J. Miller, M. Weisman, S.A. Rutledge, L.J. Barker, III, V.N. Bringi, V. Chandrasekar, A. Detwiler, N. Doesken, J. Helsdon, C. Knight, P. Krehbiel, W.A. Lyons, D. MacGorman, E. Rasmussen, W. Rison, W.D. Rust and R.J. Thomas, 2004: The Severe Thunderstorm Electrification and Precipitation Study (STEPS), *Bull. Amer. Meteor. Soc*., **85**, 1107-1125.

Lang, T.J., S.A. Rutledge and K.C. Wiens, 2004: Origins of positive cloud-to-ground lightning flashes in the stratiform region of a mesoscale convective system. *Geophys. Res. Lett.,* **31,** L10105, doi:10.1029/2004GL019823,2004.

Lyons, W.A., S.A. Cummer, M.A. Stanley, K. Wiens and T.E. Nelson, 2008: Supercells and sprites. *Bull. Amer. Meteor. Soc*. (accepted).

Lyons, W.A., 2006: The Meteorology of Transient Luminous Events – An Introduction and Overview, Chapter 1, *NATO Advanced Study Institute on Sprites, Elves and Intense Lightning Discharges*, M. Fullekrug, Ed., Corte, Corsica, 37 pp.

Lyons, W.A., L.M. Andersen, T.E. Nelson and G.R. Huffines, 2006a: Characteristics of sprite-producing electrical storms in the STEPS 2000 domain. On line summary and CD, *2nd Conf on Meteorological Applications of Lightning Data*, AMS, Atlanta, 19 pp

Lyons, W.A., S.A. Cummer and G.R. Huffines, 2006b: Characterizing intense convection using conventional and advanced lightning metrics, including charge moment change. Proc., *1st International Lightning Meteorology* Conference, Tucson, AZ. (conference CD, 31 pp).

Lyons, W.A. and S.A. Cummer, 2005: Lightning characteristics of the Aurora, NE record hail stone producing supercell of 22-23 June 2003 during BAMEX. *1st Conf. on Meteorological Applications of Lightning Data*, AMS, San Diego (available on conference preprint CD).

Lyons, W.A. and R.A. Armstrong, 2004: A review of electrical and turbulence effects of convective storms on the overlying stratosphere and mesosphere. *AMS Symposium on Space Weather,* AMS Annual Meeting, Seattle, 6 pp, CD.

Lyons, W.A., T.E. Nelson, E.R. Williams, S. A. Cummer and M.A. Stanley, 2003a: Characteristics of sprite-producing positive cloud-to-ground lightning during the 19 July STEPS mesoscale convective systems. *Mon. Wea. Rev.,* **131***,* 2417-2427.

Lyons, W.A., T.E. Nelson, R.A. Armstrong, V.P. Pasko, and M. Stanley, 2003b: Upward electrical discharges from the tops of thunderstorms. *Bull. Amer. Meteor. Soc.,* **84**, 445-454.

Lyons, W.A., M. Uliasz and T.E. Nelson, 1998b: Climatology of large peak current cloud-to-ground lightning flashes in the contiguous United States, *Mon. Wea. Rev.,* **126***,* 2217-2233.

Lyons, W.A., 1996: Sprite observations above the U.S. High Plains in relation to their parent thunderstorm systems, *J. Geophys. Res.* **101,** 29,641-29,652.

Lyons, W.A., 1994: Low-light video observations of frequent luminous structures in the stratosphere above thunderstorms. *Mon. Wea. Rev., **122,*** 1940-1946.

Pasko, V.P., U.S. Inan and T.F. Bell, 1996: Sprites as luminous columns of ionization produced by quasi-electrostatic thunderstorm fields. *Geophys. Res. Lett.,* **23**, 649-652.

Pasko, V.P., U.S. Inan and T.F. Bell, 1996: Sprites as luminous columns of ionization produced by quasi-electrostatic thundercloud fields. *Geophys. Res. Lett.*, **23**, 649-652.

Price, C., W. Burrows, P. King, 2002: The likelihood of winter sprites over the Gulf Stream. *Geophys. Res. Lett.,* **29**, doi:10.1029/2002GL015571.

Rakov, V.A. and M. A. Uman, 2003: *Lightning: Physics and Effects*. Cambridge University Press, 687 pp.

Rodger, C.J., 1999: Red sprites, upward lightning and VLF perturbations. *Reviews of Geophysics,* **37,** 317-336.

Samaras, T. and W.A. Lyons, 2008: Visualization of naturally produced lightning using high speed imaging. Preprints, *3rd Conf. on Meteorological Applications of Lightning Data,* AMS, New Orleans.

Stanley, M.A., 2000: *Sprites and their parent discharges.* Ph.D. Dissertation, New Mexico Institute of Mining Technology, Socorro, NM, 163pp.

Thomas, R.J., P.R. Krehbiel, W. Rison, S.J. Hunyady, W.P. Winn, T. Hamlin and J. Harlin, 2004: Accuracy of the Lightning Mapping Array. *J. Geophys. Res.,* **109,** D14207, doi: 10.1029/2004JD004549,2004.

van der Velde, O. A., W. A. Lyons, T. E. Nelson, S. A. Cummer, J. Li, and J. Bunnell, 2007: Analysis of the first gigantic jet recorded over continental North America, *J. Geophys. Res.,* **112***,* D20104, doi:10.1029/2007JD008575..

Williams, E.R., E. Downes, R. Boldi, W.A. Lyons and S. Heckman, 2007: The polarity asymmetry of sprite-producing lightning. *Radio Science*, **42**, Special Issue on Schumann Resonances, RS2S17, doi: 10.1029/2006RS003488.

Williams, E.R., 2001: Elves, and glow discharge tubes. *Phys. Today*, November, 41.

Williams, E.R., 1998: The positive charge reservoir for sprite-producing lightning. *J. Atmos. Sol. Terr. Phys.,* **60***,* 689-692.

Wilson, C.T.R., 1925: The electric field of a thunderstorm and some of its effects. *Proc. Phys. Soc. Lond.,* **37***,* 32D-37D.

Yashunin, S.A., E.A. Mareev and V.A Rakov, 2007: Are lightning M components capable of initiating sprites and sprite halos? *J. Geophys. Res.,* **112**, D10109, doi: 10.1029/2006JD007631.

*See author for QuickTime Illustration

Figure 1. Current state of the science regarding likelihood of various convective systems to generate the two basic classes of TLEs. (after Lyons, 2006). MCS/MCC systems are believed most prolific.

*See author for QuickTime Illustration

Figure 2. The SPRITES 2007 campaign was centered at the Yucca Ridge Field Station, Fort Collins, CO, but local measurements were supplemented by the prototype National Charge Moment Change Network and the remote Sprite Net cameras.

*See author for QuickTime Illustration

Figure 3. The two CMCN sensors in Colorado and North Carolina and local data acquisition station.

*See author for QuickTime Illustration

Figure 4. The nominal range of full coverage of each CMCN sensor (~1500 km) and typical results from the online display. The deep convection in the central U.S. is dominated by large +iCMCs (red), whereas negative events (blue) tend to be located over water on this particular day. Smaller circles and + symbols represent iCMCs with values 75 to 200 C km. Most detected iCMCs are <50 C km.

*See author for QuickTime Illustration

Figure 5. The optically confirmed TLEs during 2007 having NLDN-detected parent CGs.

*See author for QuickTime Illustration

Figure 6. The nominal area of coverage of 6 Sprite Net cameras at cooperating institutions.
The base map represents NAM WRF model output coded to emulate real time GOES imagery.

*See author for QuickTime Illustration

Figure 7. Synoptic chart for 0600 UTC 20 June 2007.

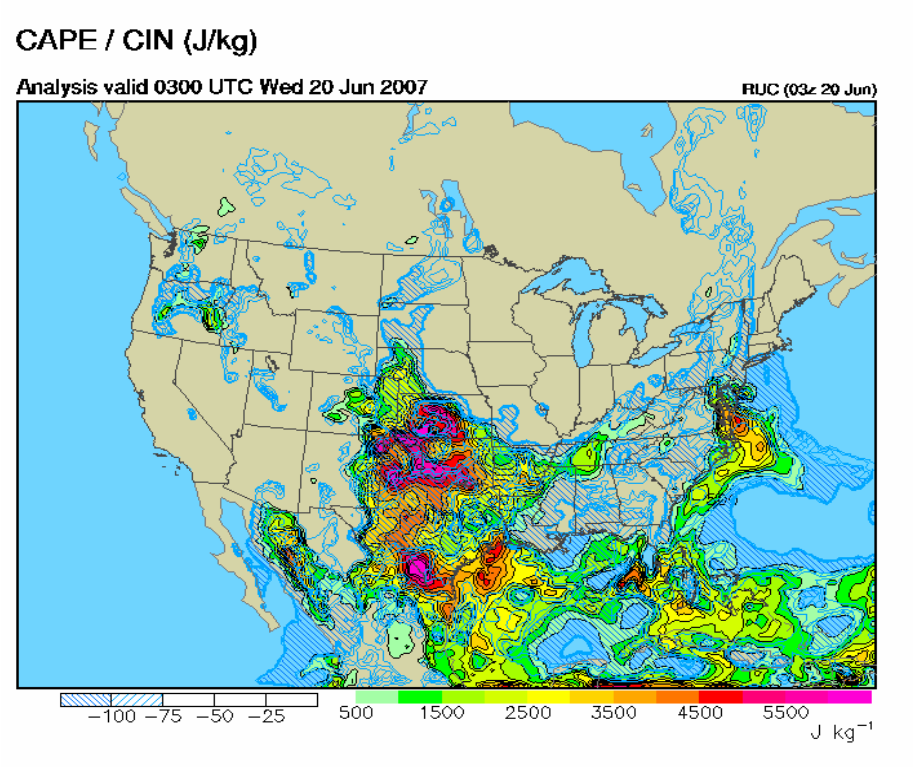

Figure 8. RUC II analysis showing extreme values of CAPE in Oklahoma at the onset of the MCC and producer of nearly 250 sprites on 20 June 2007.

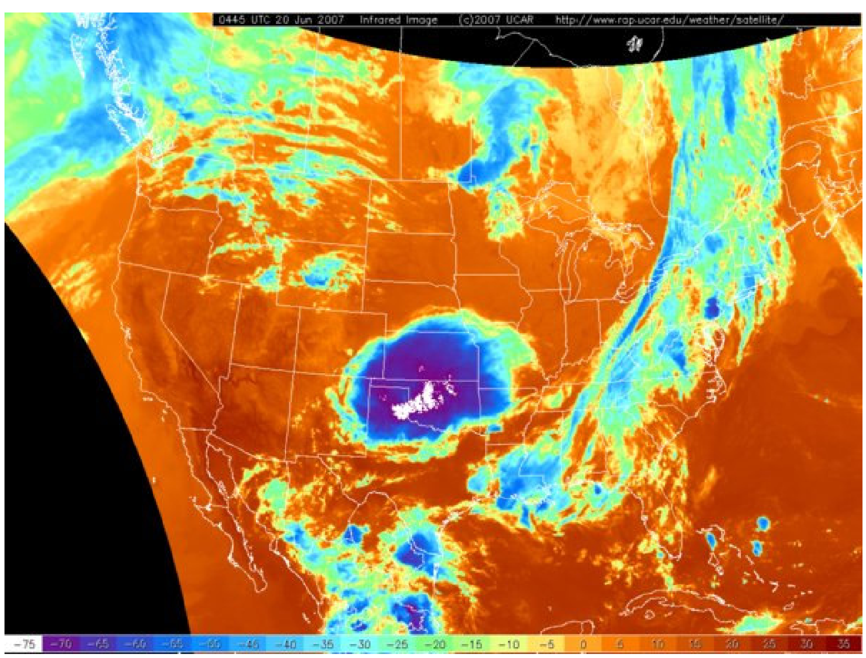

Figure 9. GOES national IR image from UCAR showing MCC developing in Oklahoma at 0445Z, 20 June 2007.

*See author for QuickTime Illustration

Figure 10. Surface reports at 0516Z 20 June 2007 showing extremely moist low level inflow into MCC.

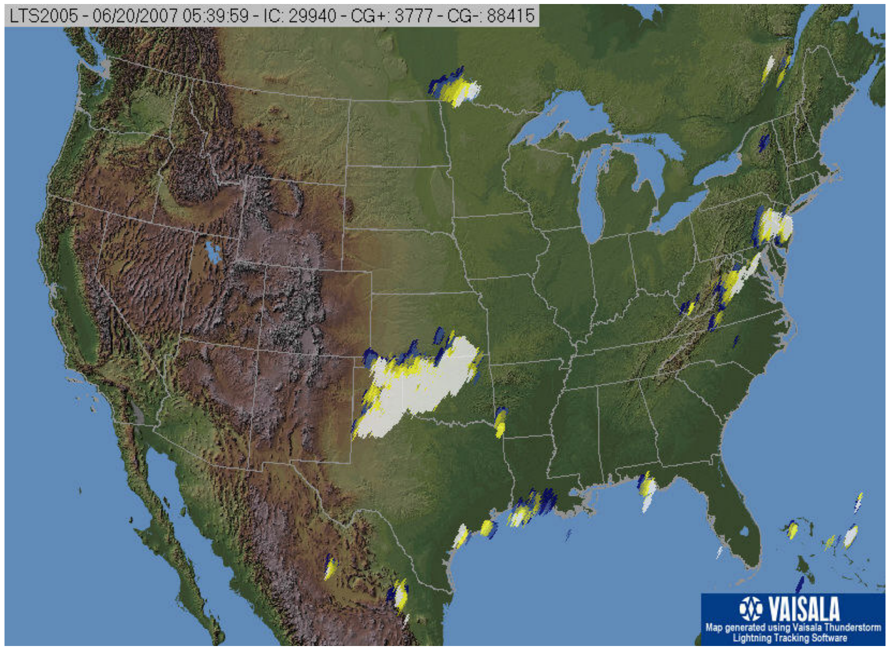

Figure 11. NLDN flash map for 0400-0600 UTC 20 June 2007.

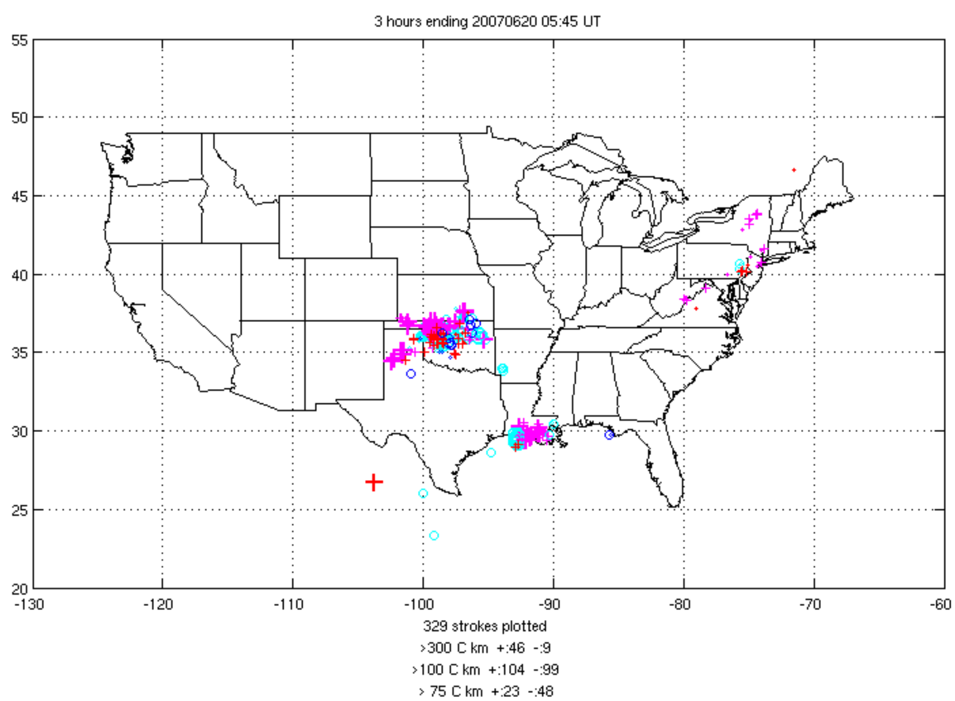

Figure 12. The National Charge Moment Change Network 3-hour summary chart at 0545 UTC 20 June 2007 reveals a large concentration of very large positive iCMC values in northern Oklahoma. However, as is typical, many storms fail to produce values even >75 C km, and very few (<<1%) CGs yield iCMC values >300 C km, a value for which TLE production probabilities, at least for +CGs, is very high.

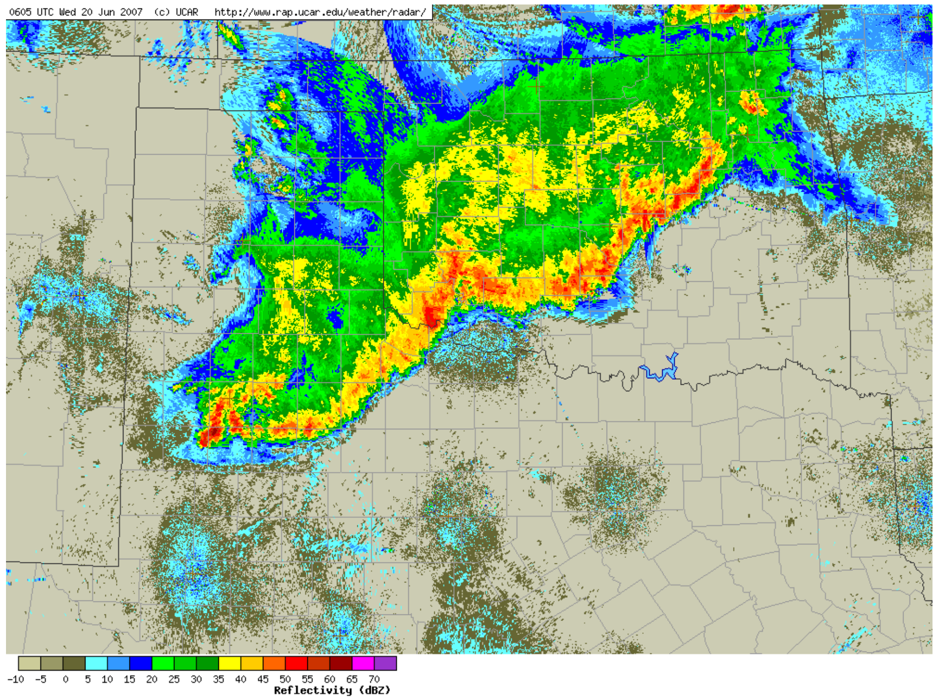

Figure 13. NEXRAD mosaic at 0605 UTC 20 June 2007 showing the classic leading edge/trailing stratiform structure of the MCC.

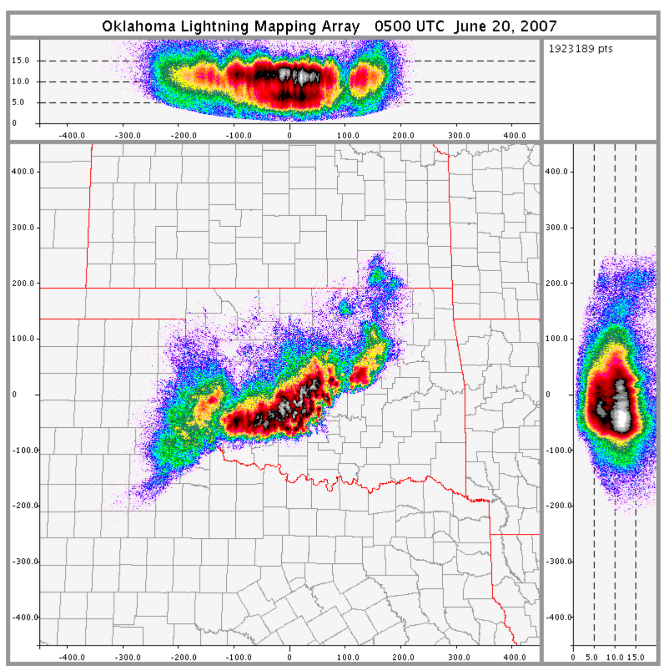

Figure 14. The Oklahoma LMA at 0500 UTC 20 June 2007 reveals intense lightning VHF sources near the leading edge of the MCC, though less active rates are found in trailing stratiform where the sprite parent +CGs tend to congregate.

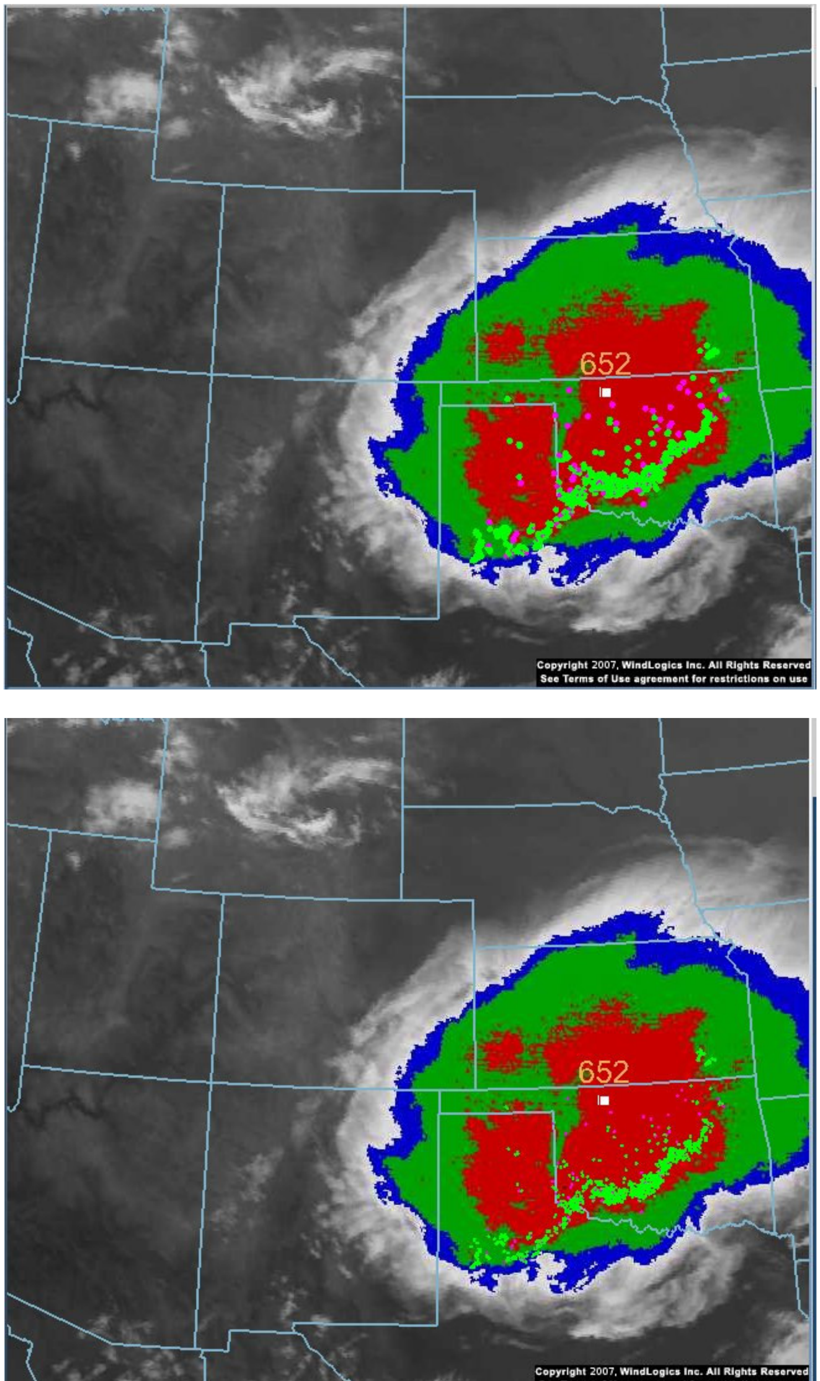

Figure 15. (a) Displays at 0600 UTC 20 June 2007 showing an enhanced GOES image, the storm centroid (white square), the –50°C canopy size (652,000 km^2) and areas of –60°C (green) and –70°C (red), and the prior 5 minutes of NLDN CGs (top), and (b) ICs (bottom) (pink positive; green negative).

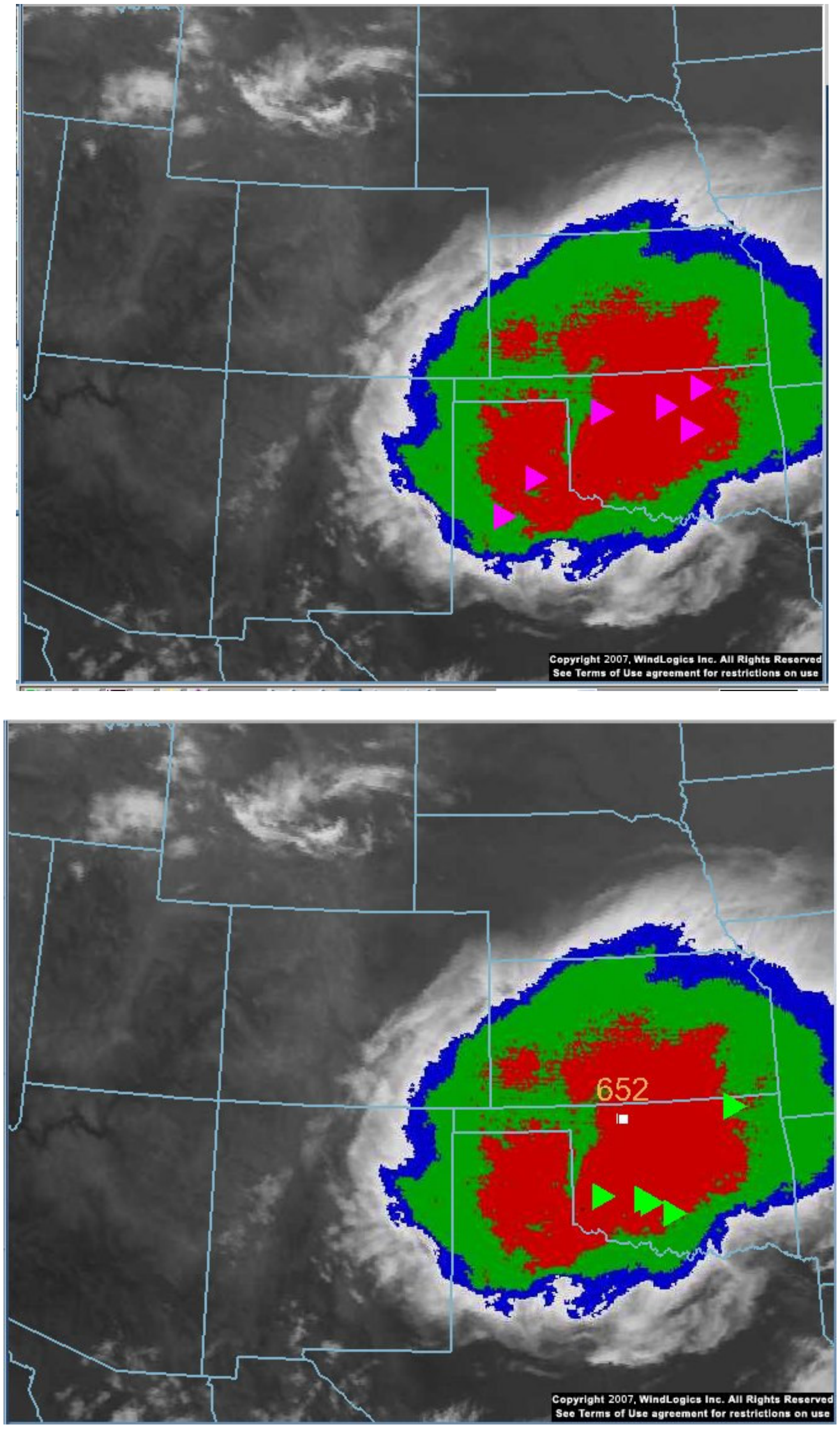

Figure 16. (a) Displays as above except with the positive CGs >75 kA (top) and (b) the negative CGs > 75 kA bottom. Note the segregation by polarity, with the positives concentrating to the rear of the southward advancing storm.

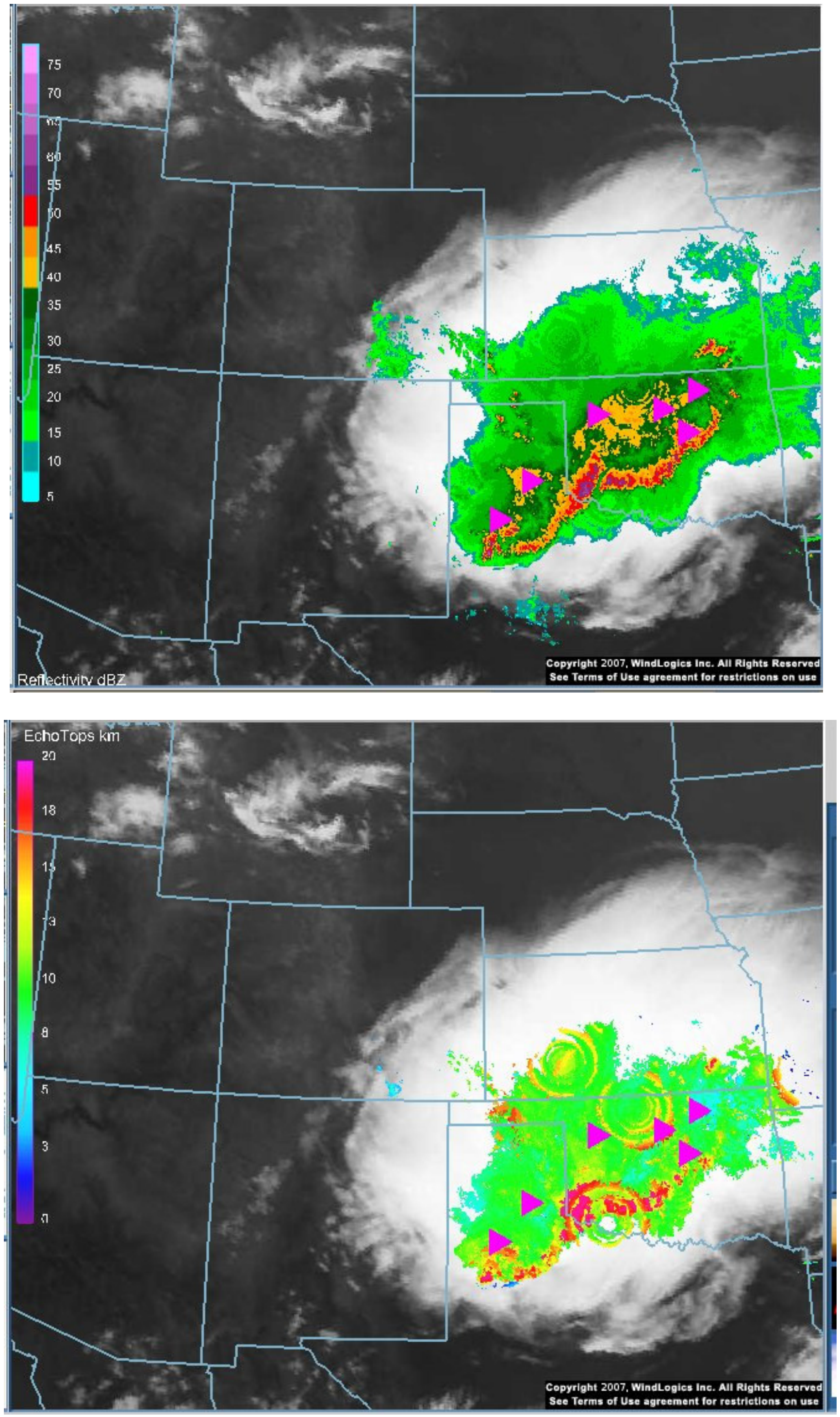

Figure 17. (a) Display at 0600 UTC 20 June 2007 showing large peak current +CGs for the preceding 5 minutes superimposed over the WDT, Inc. NEXRAD mosaic of composite reflectivity (top), and (b), echo top heights (bottom). Large positive CGs clearly concentrate in the trailing stratiform region.

*See author for QuickTime Illustration

Figure 18. Summary of the 208,736 negative CGs and 13,456 positive CGs between 0000 and 0800 UTC on 20 June 2007 (peak currents >10 kA). There were 282 optically confirmed sprites (see below).

*See author for QuickTime Illustration

Figure 19. NLDN CGs with >75 kA peak currents. As seen in the following figure, sprites +CGs tend to cluster in regions of large peak current +CGs.

*See author for QuickTime Illustration

Figure 20. Optically confirmed sprites and halos for which a parent +CG was detected by the NLDN, allowing for approximate geolocation. The actual sprite center can be offset from the +CG by up to 50 km.

*See author for QuickTime Illustration

Figure 21. (a) Plot of NLDN lightning and demarcating those detected +CGs with optically conformed sprites between 0300 and 0400 UTC 20 June 2007. and (b) Detected iCMCs > +75 C km with confirmed sprites.

*See author for QuickTime Illustration

Figure 22. Same as Fig. 21, but for 0400-0500 UTC 20 June 2007.

*See author for QuickTime Illustration

Figure 23. Same as Fig. 21, except for 0500-0600 UTC 20 June 2007.

*See author for QuickTime Illustration

Figure 24. Same as Fig. 21, except for 0600-0700 UTC 20 June 2007.

*See author for QuickTime Illustration

Figure 25. The negative iCMC events for the period 0600-0700 UTC 20 June 2007 are largely confined to the leading line convective cores having high CG lightning densities. This pattern was persistent through the storm and is commonly seen in large MCSs. Note that –CGs rarely exceed 100 C km (0.04% in this sample), and even more rarely approach the 200-300 C km range in which TLEs begin to be fairly common with +CGs, another demonstration of the sprite polarity paradox (Williams et al. 2007).

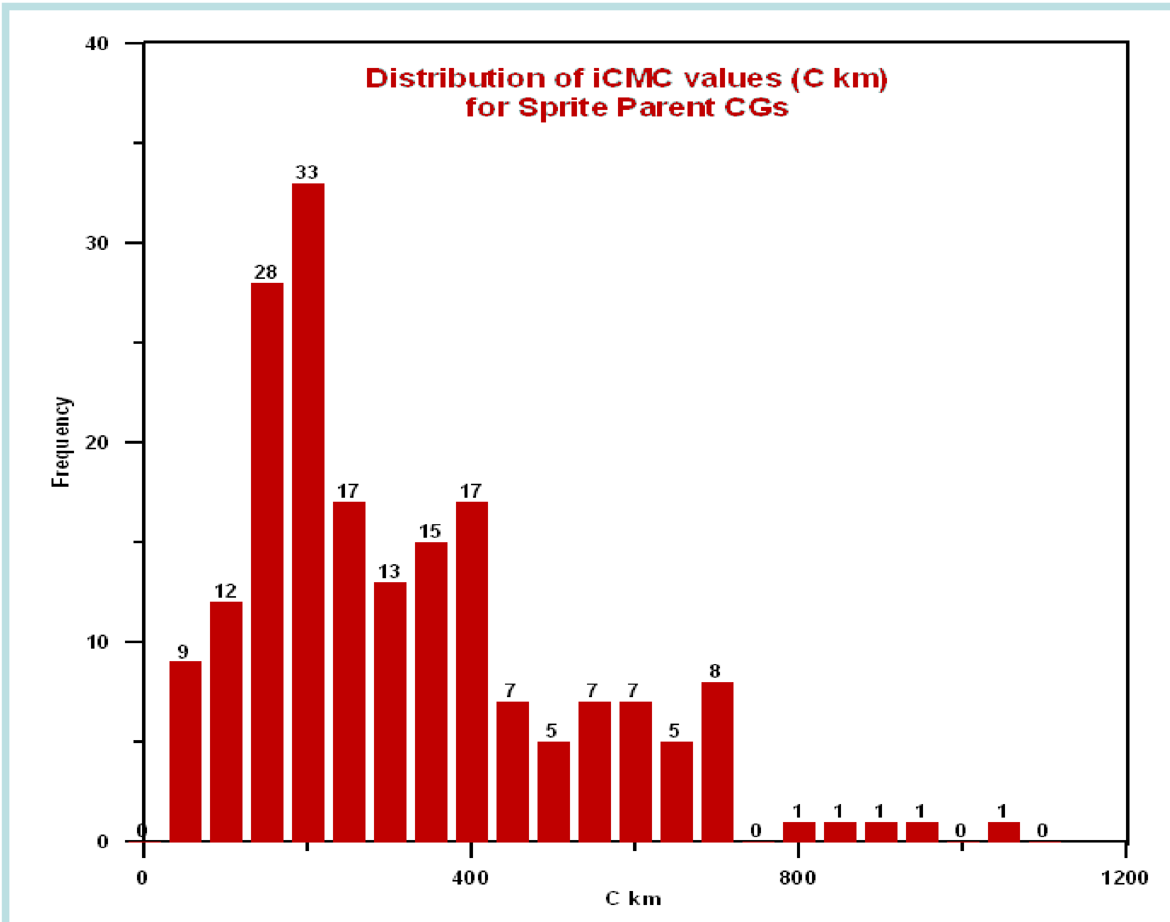

Figure 26. The values of the +iCMCs associated with the TLEs on 20 June 2007 clearly are substantially larger than those for the thousands of "normal" +CGs in this storm, typically <50 C km. The largest impulse value was over 1000 C km, with almost all sprites associated with +iCMCs > 100 C km. Events > 300 C km appear to have a > 75% chance of producing an optically detectable TLE.

*See author for QuickTime Illustration

Figure 27. The 40 largest positive iCMCs recorded by the CMCN during the period of optical observations above the MCC in Oklahoma on 20 June 2007. Of these, 30 (75%) had an optically confirmed sprite (date marked in red) as monitored from YRFS. The range of iCMCs values was from 420 to 1024 C km, all above the ~300 C km level where we suspect TLEs occur 80% or more of the time. In this instance, we note that the storm was 650 to 800 km distant and was being viewed with a line of sight with considerable light pollution near the horizon. It is likely that additional sprites occurred but were not detectable in the video record.

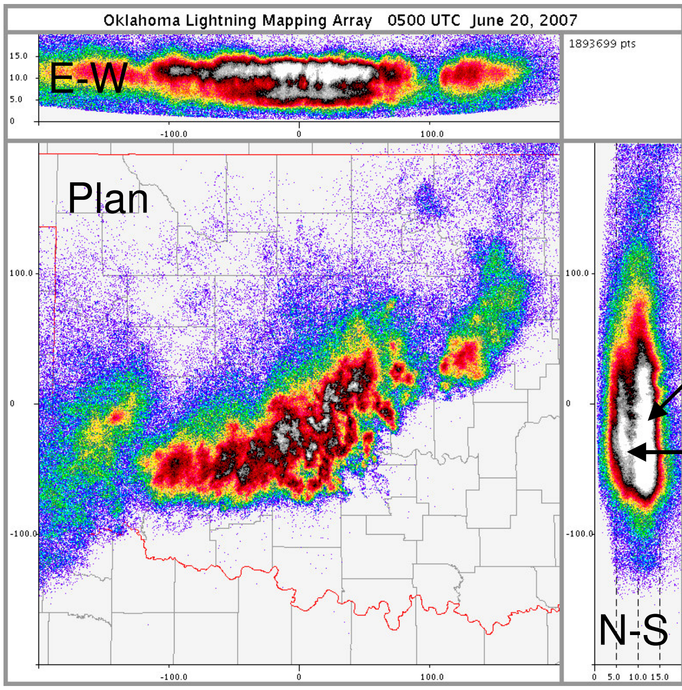

05-06 UTC
LMA Source Density

Convective Line over
LMA network

Bi-level Structure
Consistent with
Normal Tripole
(Carey et al. 2005; JGR)

Upper Density Max 11-12 km (+)
Lower Density Max 7-8 km (+)

(High resolution analysis suggests
third maximum near 4-5 km -
another positive charge layer?)

No evidence for significant
evolution during passage

<u>Norman Sounding - 00 UTC 20 Jun</u>
0 °C ~ 4.8 km MSL
-10 °C ~ 6.3 km MSL
-20 °C ~ 7.5 km MSL
-40 °C ~ 10.0 km MSL

Figure 28. An hour's worth of VHF source density from the LMA (0500-0600 UTC 20 June 2007) reveals a structure fairly typical of a tripole charge distribution, with positive charged layers mapped out around 7-8 k km and 11-12 km AGL. A possible positive charge layer was also detected around the melting layer (4-5 km).

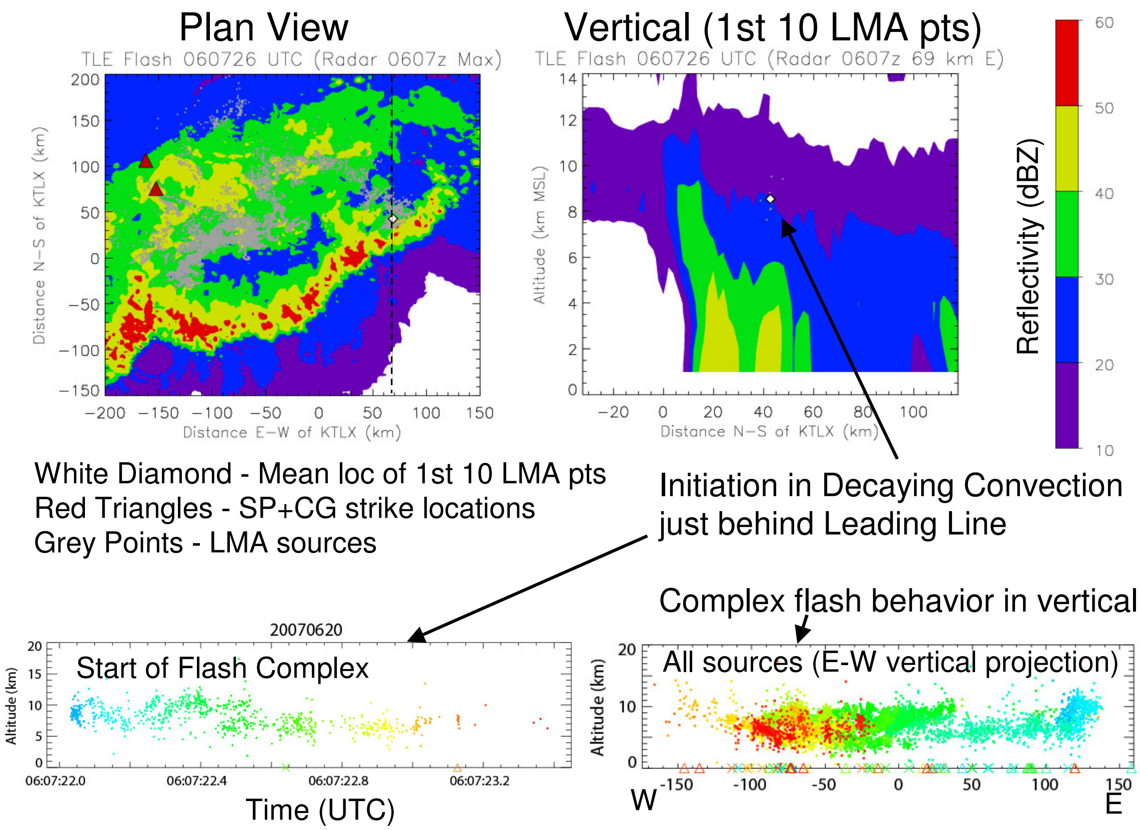

Figure 29. The gray dots plot the path of likely the longest discharge yet recorded, approaching 300 km in total length. It initiated around 8 km AGL (white dot) above a decaying convective element just behind the leading edge and then propagated rearward and downward over time. The red triangles show the +CG locations associated with the two sprites triggered by this event.

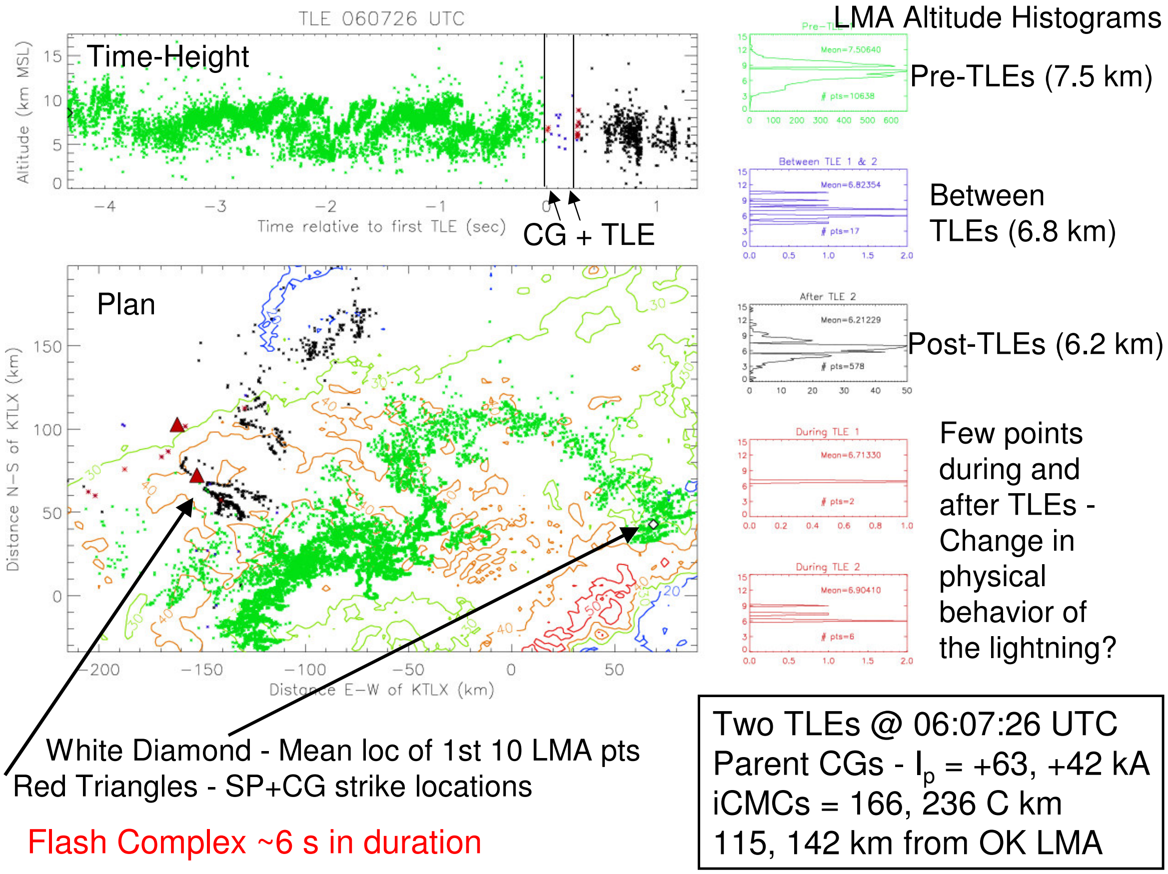

Figure 30. A close up view of the 300 km long, 6 second discharge that produced two sprites from the +CGs (red triangles) at 0607 UTC 20 June 2007.

*See author for QuickTime Illustration

Figure 31. Both positive and negative CGs produce impulse charge moment changes with values >100 C km, often approaching or even exceeding 300 C km, in the first 2 ms. Yet, for the interior of the U.S. at least, no –CG event has been associated with an optically confirmed sprite. We suggest that even though many CGs of both polarities have long continuing currents, only those for positives are of sufficient magnitude to lower the additional charge needed to induce dielectric breakdown in the mesosphere to trigger a sprite. The critical breakdown value of ~500 C km is typically reached around 10 ms (though some trigger within 2 ms, while others can be delayed > 100 ms).

*See author for QuickTime Illustration

Figure 32. Advances in high-speed imaging systems now allow obtaining video records of the many facets of the CG leader and return stroke phenomena. The top panel shows the recently discovered recoil streamers in +CGs (Samaras and Lyons 2008). In this case, video stacking sums the multiple streamers of ~100 microsecond duration. Observing the continuing current for this +CG also revealed not only its extended duration but various luminous pulses resembling M-components which have been implicated in sprite formation (Yashunin et al., 2007). Images courtesy of Tom Warner.